Loss-of-Function and Gain-of-Function Mutations in *FAB1A/B* Impair Endomembrane Homeostasis, Conferring Pleiotropic Developmental Abnormalities in Arabidopsis[1][C][W][OA]

Tomoko Hirano, Tomohiko Matsuzawa, Kaoru Takegawa, and Masa H. Sato*

Graduate School of Biostudies, Kyoto University, Kyoto 606–8501, Japan (T.H.); Laboratory of Applied Microbiology, Department of Bioscience and Biotechnology, Faculty of Agriculture, Kyushu University, Fukuoka 812–8581, Japan (T.M., K.T.); and Laboratory of Cellular Dynamics, Graduate School of Life and Environmental Sciences, Kyoto Prefectural University, Kyoto 606–8522, Japan (M.H.S.)

In eukaryotic cells, PtdIns 3,5-kinase, Fab1/PIKfyve produces PtdIns (3,5) P_2 from PtdIns 3-P, and functions in vacuole/lysosome homeostasis. Herein, we show that expression of Arabidopsis (*Arabidopsis thaliana*) *FAB1A/B* in fission yeast (*Schizosaccharomyces pombe*) *fab1* knockout cells fully complements the vacuole morphology phenotype. Subcellular localizations of FAB1A and FAB1B fused with green fluorescent protein revealed that FAB1A/B-green fluorescent proteins localize to the endosomes in root epidermal cells of Arabidopsis. Furthermore, reduction in the expression levels of *FAB1A/B* by RNA interference impairs vacuolar acidification and endocytosis. These results indicate that Arabidopsis FAB1A/B functions as PtdIns 3,5-kinase in plants and in fission yeast. Conditional knockdown mutant shows various phenotypes including root growth inhibition, hyposensitivity to exogenous auxin, and disturbance of root gravitropism. These phenotypes are observed also in the overproducing mutants of *FAB1A* and *FAB1B*. The overproducing mutants reveal additional morphological phenotypes including dwarfism, male-gametophyte sterility, and abnormal floral organs. Taken together, this evidence indicates that imbalanced expression of *FAB1A/B* impairs endomembrane homeostasis including endocytosis, vacuole formation, and vacuolar acidification, which causes pleiotropic developmental phenotypes mostly related to the auxin signaling in Arabidopsis.

In eukaryotic cells, phosphoinositides play important roles in various cellular signaling processes and in membrane trafficking by functioning as regulatory components through recruitment of protein effectors to the sites of action (Odorizzi et al., 1998). Among various phophoinositides, phosphatidylinositol 3-P (PtdIns3P) and phosphatidylinositol 3,5-bisphosphate (PtdIns [3,5]P_2) function in endosomal trafficking by regulated endocytosis and protein sorting to the vacuole/lysosome via the endosomes, respectively (Gary et al., 1998; Odorizzi et al., 1998). PtdIns3P exists on early endosomes and inside of multivesicular bodies (MVBs), whereas PtdIns (3,5)P_2 is present on the external membrane of MVBs (Odorizzi et al., 1998). PtdIns3P is generated from phosphatidyinositol (PI) by class III PI3-kinase, Vps34p; subsequently, PtdIns (3,5)P_2 is produced from PtdIns3P by PtdIns3P 5-kinase, Fab1p/PIKfyve, in various eukaryotic cells including yeasts, animals, and plants (Efe et al., 2005).

In yeast (*Saccharomyces cerevisiae*), the *fab1* mutant shows an enlarged vacuolar phenotype. It is defective in terms of vacuolar acidification, osmoregulation, and inheritance of vacuoles, and exhibits a growth defect at high temperatures (Gary et al., 1998; Odorizzi et al., 1998). Functionally, ScFab1p is necessary both for retrograde vesicle transport from vacuoles to endoplasmic reticulum (ER)/Golgi and for the sorting of cell membrane-integrated proteins in MVBs (Gary et al., 1998; Odorizzi et al., 1998; Shaw et al., 2003). Fission yeast (*Schizosaccharomyces pombe*) also has a Fab1p homolog (designated as SpFab1p), which restores the PtdIns (3,5)P_2 deficiency in *Scfab1* disruptant cells (McEwen et al., 1999). The fission yeast *fab1* mutant also has an enlarged vacuolar structure (Morishita et al., 2002). The mammalian ortholog of Fab1p is designated as PIKfyve. Like Fab1p in yeast, PIKfyve is also necessary for endomembrane homeostasis. Overexpression of a dominant kinase-inactive mutant exhibits an enlarged lysosome phenotype (Ikonomov

[1] This work was supported by a grant from the Japanese Ministry of Education, Culture, Sports, Science and Technology, a grant-in-aid for Basic Science Research (C), and by Strategic Research Funds of Kyoto Prefectural University (to M.H.S.).

* Corresponding author; e-mail mhsato@kpu.ac.jp.

The author responsible for distribution of materials integral to the findings presented in this article in accordance with the policy described in the Instructions for Authors (www.plantphysiol.org) is: Masa H. Sato (mhsato@kpu.ac.jp).

[C] Some figures in this article are displayed in color online but in black and white in the print edition.

[W] The online version of this article contains Web-only data.

[OA] Open Access articles can be viewed online without a subscription.

www.plantphysiol.org/cgi/doi/10.1104/pp.110.167981

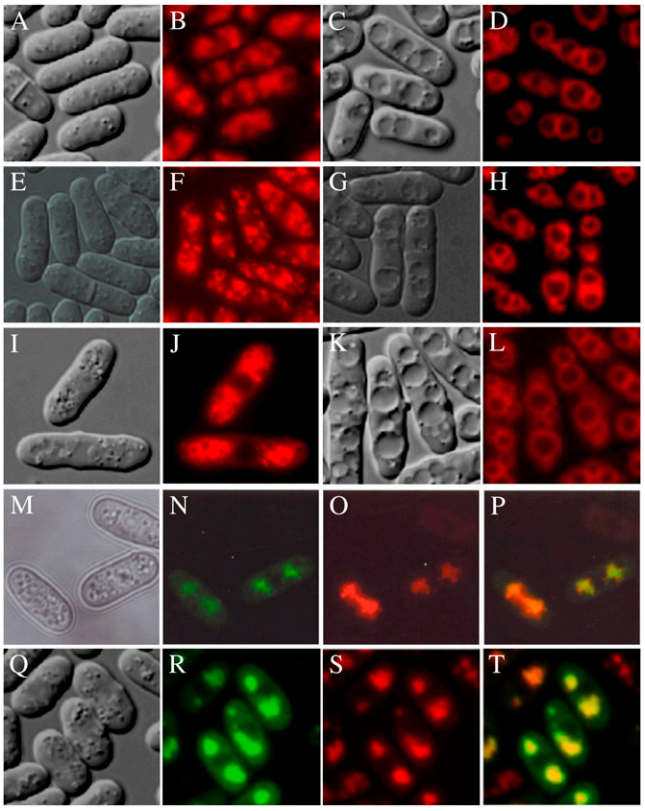

Figure 1. Arabidopsis *FAB1A* and *FAB1B* complement the vacuolar morphology phenotype of *ste12* mutant in fission yeast. Wild-type cells with pREP41 empty vector (A and B), *ste12* cells with pREP41 (C and D), *ste12* cells with FAB1A/pREP41 in the absence of thiamine (E and F), or in the presence of thiamine (G and H), *ste12* cells with FAB1B/pREP41 in the absence of thiamine (I and J), or in the presence of thiamine (K and L). Vacuolar shapes were visualized by staining with FM4-64 (B, D, F, H, J, L, O, and S), and creating DIC images (A, C, E, G, I, K, M, and Q). In *ste12* cells expressed FAB1A-GFP: DIC image (M), fluorescence of FAB1A-GFP (N), FM4-64 staining (O), merged image of N and O (P); and in those expressed FAB1B-GFP: DIC image (Q), fluorescence of FAB1A-GFP (R), FM4-64 staining (S), merged image of N and O (T) were observed.

et al., 2001). Consequently, a shared feature of Fab1p/PIKfyve mutants in yeasts and animals is the formation of swollen vacuolar/lysosomal structures, suggesting the presence of a conserved function for Fab1p/PIKfyve in the regulation of endomembrane homeostasis (Efe et al., 2005).

In Arabidopsis (*Arabidopsis thaliana*), four genes encoding putative Fab1p/PIKfyve proteins, *FAB1A* (At4g33240), *FAB1B* (At3g14270), *FAB1C* (At1g71010), and *FAB1D* (At1g34260), were identified in the genome. Among the four FAB1/PIKfyve orthologs, only FAB1A and FAB1B contain a predicted FYVE domain, which is conserved though all FAB1 orthologs, at their N termini. Although the functions of FAB1C and FAB1D are unknown, FAB1A and FAB1B reportedly possess a redundant function in male gametophyte development. Because of the male gametophyte lethal phenotype of the *fab1a/fab1b* double-knockout Arabidopsis plant, the function of Fab1p/PIKfyve proteins in vegetative tissues remains largely unknown, although both *fab1a* and *fab1b* homozygous single-mutant plants exhibited a leaf-curl phenotype (Whitley et al., 2009).

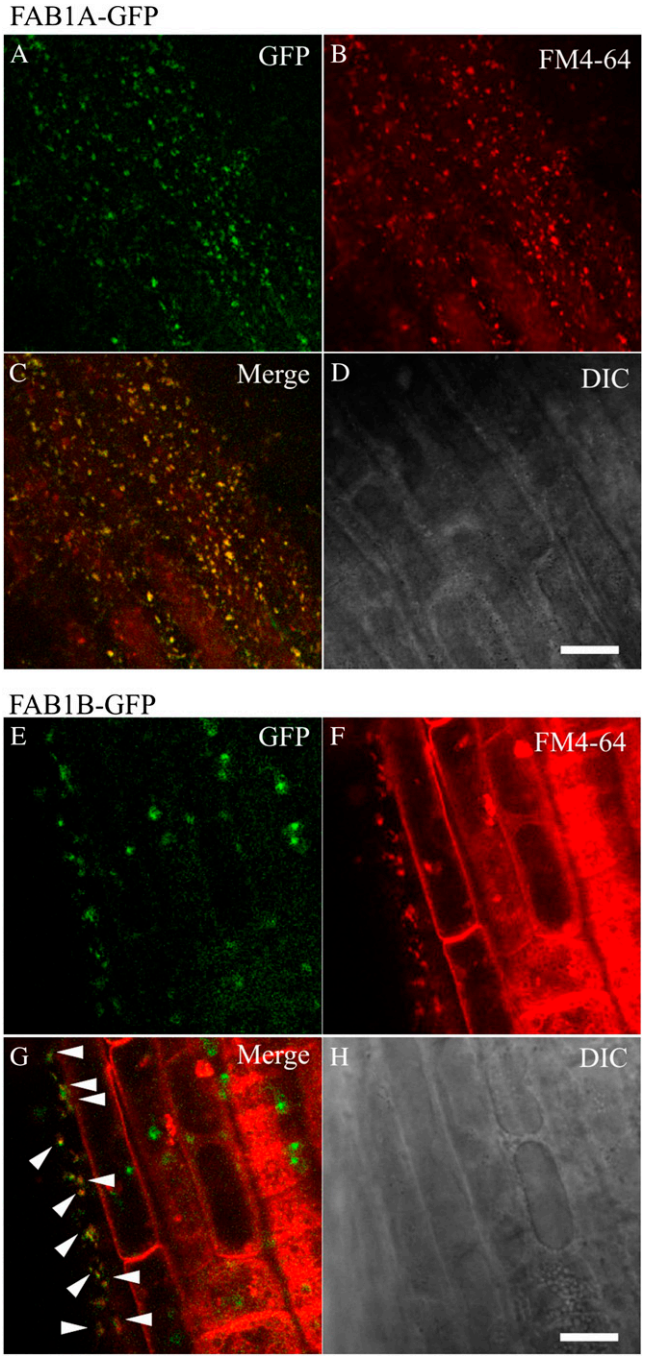

Figure 2. Localization patterns of Fab1A/B-GFPs in root epidermal cells. Five-day-old seedlings of the transgenic plant expressing FAB1A-GFP and FAB1B-GFP were observed using confocal microscopy. FAB1A-GFP expressed in root epidermal cells (A), stained by FM4-64 (B), merged image of A and B (C), and DIC image (D) are shown. FAB1B-GFP expressed in root epidermal cells (E), stained by FM4-64 (F), merged image of A and B (G), and DIC image (H) are shown. Arrowheads indicate the merged dot structures. Bars = 10 μm.

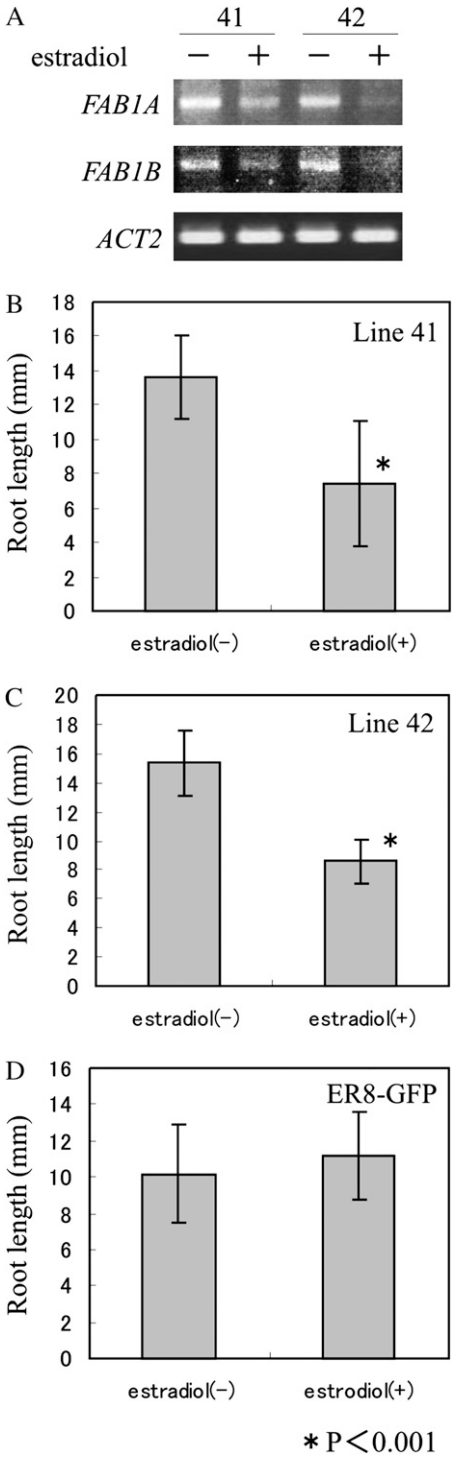

Figure 3. Decreased expression of *FAB1A* and *FAB1B* inhibits root growth. A, Expressions of *FAB1A* and *FAB1B* in lines 41 and 42 were measured using semiquantitative RT-PCR in the presence or absence of estradiol. The expression of *ACT2* (At3g18780) was used as an internal standard. The lengths of roots of the lines 41 (B) and 42 (C) were measured in the 5-d-old seedlings after induction. D, Transgenic plants expressing GFP under control of an estradiol-inducible promoter were used as a mock control. Bars show mean values ± SDS (number of roots measured: line 41 − estradiol, $n = 20$; line 41 + estradiol, $n = 18$; line 42 − estradiol, $n = 28$; line 42 + estradiol, $n = 31$; ER8-GFP − estradiol, $n = 28$; ER8-GFP + estradiol, $n = 22$). Asterisks denote statistically significant differences in the length of root of each line compared with uninduced condition (*$P < 0.001$; Student's *t* test).

In this study, we attempt to address the role of Fab1p/PIKfyve proteins by analyzing the phenotypes of inducible artificial microRNA (amiRNA) mutants and constitutive or inducible gain-of-function mutants of *FAB1A* and *FAB1B*. Our results demonstrated that Fab1p/PIKfyve protein is important for endomembrane homeostasis including endocytosis, vacuole formation, and vacuolar acidification. Moreover, defective FAB1 function causes pleiotropic developmental abnormalities in Arabidopsis.

RESULTS

Arabidopsis FAB1A and FAB1B Complement the Enlarged Vacuolar Phenotype of the Fission Yeast *ste12*Δ Mutant

In fission yeast, *ste12*+ gene encodes PtdIns3P 5-kinase, known as SpFab1p. The *ste12*Δ mutant in fission yeast shows an aberrant swollen vacuole phenotype resembling that of yeast (Morishita et al., 2002).

Arabidopsis FAB1A and FAB1B share 14.2% amino acid sequence homology with SpFab1p. To test whether FAB1A and FAB1B have an ability to function as PtdIns3P 5-kinase in fission yeast, we expressed Arabidopsis FAB1A and FAB1B in the *ste12*Δ mutant under control of the fission yeast *nmt* promoter. The wild-type cell-transformed pREP41 empty vector had many small vacuoles (Fig. 1, A and B), but the *ste12* cell-transformed pREP41 empty vector had a few enlarged vacuoles (Fig. 1, C and D). *FAB1A* on pREP41 was introduced into *ste12* cells (Fig. 1, E–H). When *FAB1A* was expressed under control of the thiamine-repressible *nmt1* promoter in pREP41, in the *ste12* mutant, the morphology of the vacuoles changed from an enlarged shape (Fig. 1, G and H) to normal small vacuoles (Fig. 1, E and F) like those in wild-type cells. The *ste12* cells conditionally expressing FAB1B also had small vacuoles (Fig. 1, I and J) similar to those in wild type, although *ste12* cells, which repress expression of FAB1B by adding 10 μg/mL thiamine, had abnormal enlarged vacuoles (Fig. 1, K and L). When C-terminal GFP-fused FAB1A and FAB1B (designated as FAB1A-GFP and FAB1B-GFP, respectively) were expressed in *ste12*Δ cells, the enlarged vacuolar morphology of *ste12*Δ cells changed to small vacuoles like those observed in wild-type cells (Fig. 1, M and Q), indicating that both FAB1A-GFP (Fig. 1 M–P) and FAB1B-GFP (Fig. 1, Q–T) fully complemented the *ste12* phenotype of the vacuolar morphology. The GFP fluorescence of these fusion proteins was merged completely with FM4-64-labeled fragmented vacuoles (Fig. 1, N–P and R–T), indicating that ectopically expressed FAB1A-GFP and FAB1B-GFP localized on the vacuolar membrane of fission yeast. These data

illustrate that Arabidopsis FAB1A and FAB1B function as PtdIns 3P-5 kinase in fission yeast.

FAB1A/B-GFPs Localize to Endosomes in Arabidopsis Root Cells

To determine the subcellular localizations of FAB1A/B proteins, we generated transgenic Arabidopsis plants expressing GFP-fused FAB1A or FAB1B (FAB1A-GFP, FAB1B-GFP) under control of their native promoters. Then, we observed the subcellular localizations of these proteins in root cells.

In epidermal cells in the root differentiation zone, the fluorescence of FAB1A-GFP localized to punctate structures throughout the cytosol (Fig. 2A). Most of these punctate structures overlapped with FM4-64-labeled endosomal compartments, implying that FAB1A-GFP localized to the endosomes of root epidermal cells (Fig. 2, B and C). In addition, FAB1B-GFP exhibited identical localization patterns to those of FAB1A-GFP (Fig. 2, E–G). These data revealed that FAB1A and FAB1B localize to the endosomes in Arabidopsis root epidermal cells.

Knockdown Lines of *FAB1A/B* Exhibit a Root Growth Inhibition Phenotype

In the previous study, the functions of *FAB1A* and *FAB1B* genes were analyzed using the T-DNA insertional mutation lines of both genes in Arabidopsis. Although genetic transmission analysis revealed a failure in generating the double-mutant lines because of inviability of the pollens carrying mutations in both *FAB1A* and *FAB1B* genes, the single-homozygous mutants of both genes exhibited a weak morphological phenotype in which the leaves are curled slightly (Whitley et al., 2009).

To examine the physiological function of FAB1A/B in vegetative tissues, we generated conditional knockdown mutant plants using the amiRNA technique (Alvarez et al., 2006; Niu et al., 2006; Schwab et al., 2006; Warthmann et al., 2008). AmiRNAs, which are normally absent in plants, are artificially designed 12-mer single-stranded RNAs. The amiRNAs specifically down-regulate not only a single target, but also multiple protein-coding genes having similar sequences (Schwab et al., 2006; Ossowski et al., 2008). We computed optimal amiRNA sequences for only attenuating *FAB1A* and *FAB1B* expression simultaneously using software (WMD version 3; http://wmd.weigelworld.org/). The target amiRNA sequences were introduced into the pER8 vector, which can induce the gene expression under control of the artificial 17-β-estradiol-inducible promoter (Zuo et al., 2000).

The amiRNA transgenic lines were grown for 5 d on one-half-strength Murashige and Skoog agar plates in the presence or absence of 10 μM estradiol. Then the root lengths were measured. Decreased expression of *FAB1A* and *FAB1B* transcripts in the transgenic plants grown in the presence of estradiol was confirmed using semiquantitative reverse transcription (RT)-PCR. In the presence of estradiol, the expressions of *FAB1A* and *FAB1B* were attenuated in transgenic lines 41 and 42. Particularly, the expression levels of both genes were strongly inhibited in line 42 (Fig. 3A).

In the presence of estradiol, the root lengths in lines 41 and 42 were considerably shortened (Fig. 3, B and C). In particular, the root growth inhibition in the presence of estradiol was significant in line 42, suggesting that the decreased expression of *FAB1A* and *FAB1B* correlated with the root growth inhibition in an

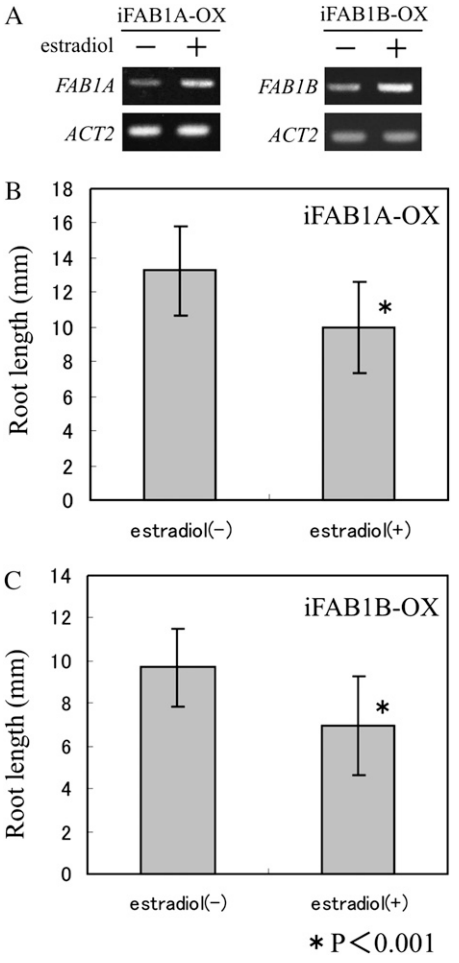

Figure 4. Overexpressions of *FAB1A* and *FAB1B* inhibits root growth. Two-day-old seedlings of the transgenic plants grown on one-half-strength Murashige and Skoog plates were transferred to one-half-strength Murashige and Skoog plates with or without 10 μM estradiol. After 5 d, the expression levels and lengths of roots were measured. A, The expression levels of *FAB1A* and *FAB1B* were measured using semiquantitative RT-PCR. *ACT2* was used as an internal standard. The root lengths of lines overexpressing *FAB1A* (B) and *FAB1B* (C) were measured 5 d after induction. Bars represent mean values ± SD (numbers of roots measured: iFAB1A-OX − estradiol, n = 43; iFAB1A-OX + estradiol, n = 48; iFAB1B-OX − estradiol, n = 19; iFAB1B-OX + estradiol, n = 15). Asterisks denote statistically significant differences in the length of root of each line compared with uninduced condition (*$P < 0.001$; Student's t test).

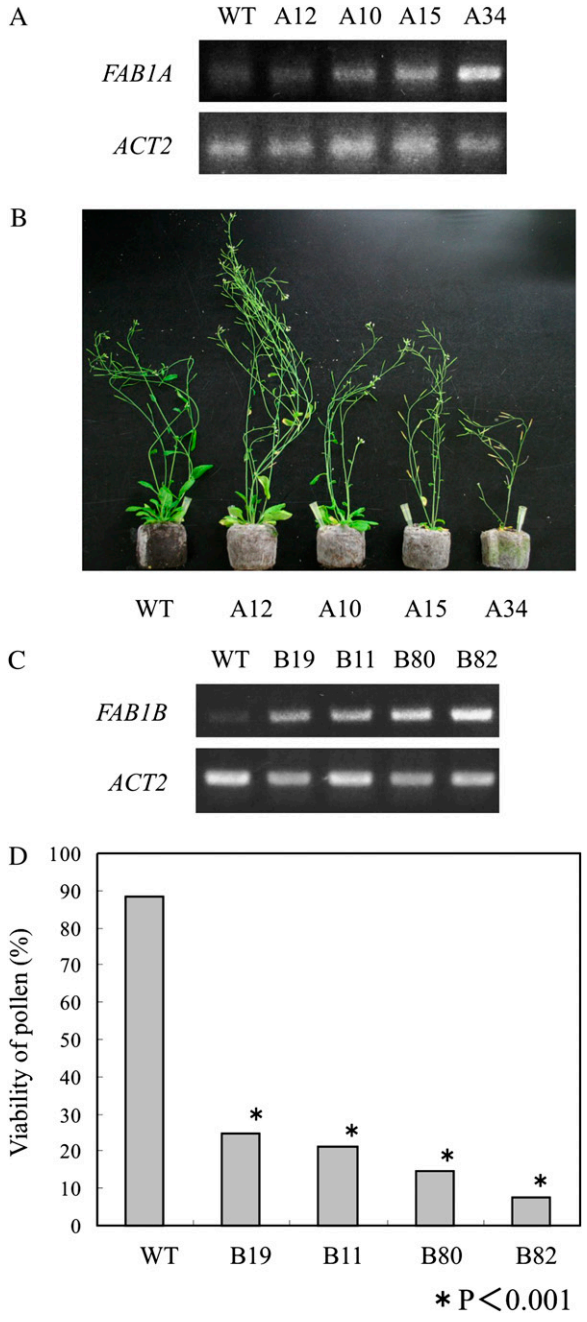

Figure 5. *FAB1A/B* overexpressing plants become dwarfed and sterile dose dependently. A, Expression levels of four independent lines of *FAB1A* with different expression levels (lines A12, A10, A15, and A34) were measured using semiquantitative RT-PCR analysis with *ACT2* as an internal standard. B, Sizes of 30-d-old transgenic plants: The lengths of shoots of the transgenic plants became dwarfed as the expression level of *FAB1A* increased. C, Expression levels of the four transgenic lines expressing *FAB1B* (lines B11, B19, B80, and B82) were measured using semiquantitative RT-PCR. D, Viability of pollen from these transgenic plants was measured by counting the FDA-stained pollen grains. The pollen grains of four lines and the wild type were stained with FDA. Grains exhibiting FDA fluorescence were counted (number of grains counted: wild type, $n = 152$; line B19, $n = 233$; line B11, $n = 385$; line B80, $n = 245$; line B82, $n = 225$). Asterisks denote statistically significant differences in the viability of pollen of each line compared with wild type (*$P < 0.001$; Student's t test). [See online article for color version of this figure.]

expression dose-dependent manner in Arabidopsis. The lengths of root hairs in line 42 were also shortened considerably compared with the uninduced condition (Supplemental Fig. S1). No growth inhibitions of root and root hair were observed in the control plant, which exogenously expressed GFP in the presence of estradiol (Fig. 3D; Supplemental Fig. S1).

Overexpression Lines of *FAB1A/B* Also Exhibit a Root Growth Inhibition Phenotype, Dwarfism, and Decreasing Viability of Pollen

To elucidate the effect of overexpression of *FAB1A/B* genes in root growth, we generated transgenic plants (43 lines for iFAB1A-OX and 34 lines for iFAB1B-OX) that were able to induce the expression of *FAB1A* or *FAB1B* in the presence of estradiol. We chose one overexpression line from each gene and analyzed whether root growth inhibition occurred when each gene was overexpressed. When both *FAB1A* and *FAB1B* were overexpressed in the presence of estradiol (Fig. 4A), the roots of *FAB1A*-expressed or *FAB1B*-expressed plants were shortened considerably (Fig. 4, B and C), indicating that overexpression of *FAB1A/B* created an inhibitory effect on the root elongation similar to that caused by the loss of function of the genes. Similar to the case of the knockdown lines, the growth inhibition of root hairs in *FAB1A*-overexpressed or *FAB1B*-overexpressed plants induced by estradiol was also observed (Supplemental Fig. S1).

If the expression levels of *FAB1A* and *FAB1B* affect root elongation, then it might be expected that shoot development is also inhibited by overexpression of these genes. To test this possibility, the degrees of growth of several constitutive overexpression lines of *FAB1A* with various expression levels were compared. As shown in Figure 5, A and B, the shoots of the constitutive overexpression lines of *FAB1A* (cFAB1A-OX) were dwarfed increasingly as the expression level of the gene increased. A similar dwarf phenotype was also observed in constitutive *FAB1B* overexpression lines (data not shown).

Additionally, of the 39 constitutive overexpression lines of *FAB1A*, five exhibited a sterility phenotype (data not shown). It was reported previously that crossing the mutant lines of *FAB1A* and *FAB1B* produced no homozygous double-mutant seeds because of a maturation defect in *fab1a/b* double-homozygous mutant pollens (Whitley et al., 2009). Therefore, it is likely that the sterility phenotype of the constitutive overexpression lines of *FAB1A/B* occurred for the same reason.

To test the viability of pollen grains, we measured the number of living pollen via the fluorescein diacetate (FDA) staining method in several cFAB1B-OX lines with a severe sterile phenotype (Fig. 5D); the

expression levels of these lines were examined using RT-PCR (Fig. 5C). The pollen viability was decreased depending on the expression level of *FAB1B*, indicating that overexpression of *FAB1* negatively affected the pollen viability (Fig. 5, C and D). The viability of pollen of cFAB1A-OX was also correlated with the expression levels of FAB1A (data not shown).

Whitley et al. (2009) reported that pollens of *fab1a/fab1b* double-homozygous mutant display an abnormal vacuolar phenotype in the late pollen development. We examined whether the inviability of pollens in *FAB1A/B* overexpression lines was caused by abnormal vacuole formation during pollen development by the neutral red staining. After staining, the vast majority of pollens had aberrant large vacuoles in both *FAB1A* and *FAB1B* overexpression lines, although pollen grains from wild-type plant showed numerous small vacuoles with uniform sizes (Supplemental Fig. S2), indicating that inviability of pollens in the overexpression lines resulted from the vacuole formation defect that is also observed in *fab1a/fab1b* double-homozygous mutant pollens.

Reduction in *FAB1A/B* Expression Causes Severe Defects in Vacuole Acidification and Endocytosis

Typical features of Fab1p/PIKfyve mutants in yeasts and animals are defective in vacuole acidification, fluid phase endocytosis, and formation of normal vacular/lysosomal structures (Gary et al., 1998; Odorizzi et al., 1998; McEwen et al., 1999; Ikonomov et al., 2001). To elucidate whether the cellular phenotypes of knockdown and overexpressing mutants of *FAB1A/B* resemble those in yeast and animal cells, we assessed vacuole acidification and endocytosis using an acidification marker (acridine orange) and a fluorescent endocytosis marker (FM4-64).

Results show that conditional knockdowns of *FAB1A* and *FAB1B* (Fig. 6B), overexpression of *FAB1A* (Fig. 6D) or *FAB1B* (Fig. 6F) severely impaired the acidification of the central vacuoles compared with noninduced plants (Fig. 6, A, C, and E). However the punctate structures inside the cells were still acidified in the presence of estradiol in these mutants. Probably, these punctate structures are the endosomes (Fig. 6, B, D, and F).

Endocytosis of FM4-64 was severely delayed in the presence of estradiol (Supplemental Fig. S3). After 1 min labeling, fluorescence of FM4-64 was observed within the inside of the root cells (Supplemental Fig. S3A), although these intracellular structures were never observed in the presence of estradiol (Supplemental Fig. S3B). After 120 min in the mutant cells, the endosomes were labeled but the vacuolar membrane was not labeled yet in the presence of estradiol (Supplemental Fig. S3F), although the vacuolar membranes of the control cells were fully labeled with the dye (Supplemental Fig. S3E).

These results show that the cellular phenotypes of Arabidopsis *fab1* mutants are similar to those in other eukaryotic cells.

Auxin-Signaling Phenotypes of Knockdown and Overexpression Mutants of *FAB1A/B*

Reportedly, both *fab1a/fab1a* and *fab1b/fab1b* double-homozygous mutant lines revealed a leaf-curling phenotype in rosette leaves (Whitley et al., 2009). This leaf-curling phenotype is known as a typical phenotype of the auxin-resistant mutants in Arabidopsis (Hobbie and Estelle, 1995). Therefore, we investigated whether the *FAB1A/B* knockdown and overexpression mutants can be expected to alter the sensitivity to exogenous auxin. First, we investigated auxin-dependent lateral root formation in these mutants, which is a typical auxin-responsive phenotype in Arabidopsis. The 4-d-old seedlings grown on one-half-strength Murashige and Skoog agar plate were transferred on

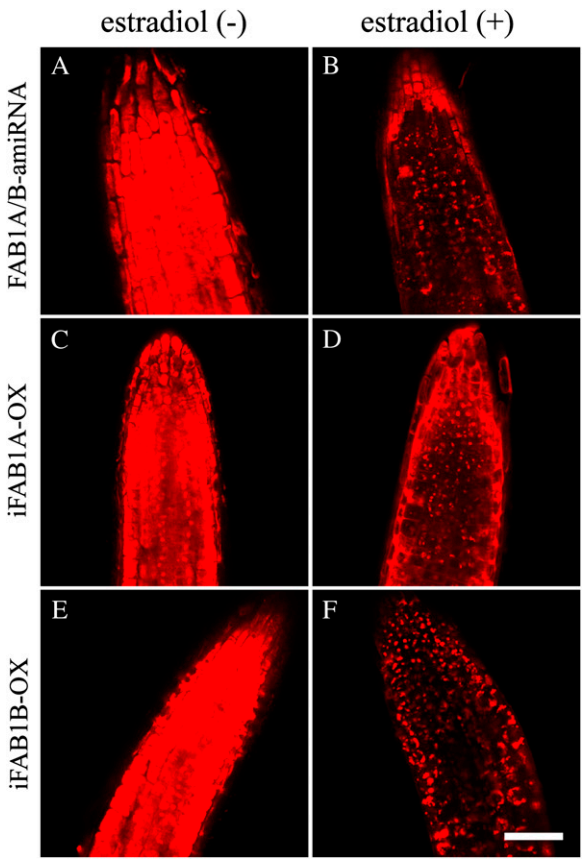

Figure 6. Reduction of *FAB1A/B* and overexpression of *FAB1A* or *FAB1B* cause acidification defect of central vacuoles of the root epidermal cells. Root epidermal cells of 5-d-old seedlings of FAB1A/B-amiRNA (A and B) or iFAB1A-OX (C and D) and iFAB1B-OX (E and F) lines were stained with acridine orange. Fluorescence was observed using confocal microscopy. The root epidermal cells in which reduction of *FAB1A/B* expression (B), overexpression of *FAB1A* (D), and overexpression of *FAB1B* (F) were induced in the presence of estradiol. Although the central vacuoles were fully acidificated in the root epidermal cells of noninduced FAB1A/B-amiRNA line (A), iFAB1A-OX line (C), and iFAB1B-OX line (E), no acidification inside of the central vacuole was observed in each line of cells (B, D, and F). Bar = 50 μm. [See online article for color version of this figure.]

one-half-strength Murashige and Skoog plates with or without 0.1 μM 2,4-dichlorophenoxyacetic acid (2,4-D). After day five, the numbers of lateral roots of the mutants were counted.

In the absence of estradiol, the lateral roots of the amiRNA plant (line 42 in Fig. 3) increased when 0.1 μM 2,4-D was added to the medium, indicating that the transgenic plant is sensitive to auxin when the gene expressions of *FAB1A/B* were not inhibited. However, in the presence of estradiol, the addition of 2,4-D did not produce additional lateral roots (Fig. 7A), indicating that sensitivity to auxin in this line decreased strongly when the expressions of *FAB1A/B* were inhibited. Similarly, in the presence of estradiol, the induction of the lateral roots in the *FAB1A* or *FAB1B* overexpression lines was reduced significantly with the addition of 0.1 μM 2,4-D, implying that each overexpression line became less sensitive to auxin (Fig. 7, B and C). The induction of the lateral roots in the mock control, the inducible GFP expression line (ER8-GFP), with 0.1 μM 2,4-D was unaffected by the presence of estradiol (Fig. 7D).

Next, we tested whether the root gravitropic response was changed when the expressions of *FAB1A* and *FAB1B* were increased or decreased conditionally. The transgenic plants were grown on horizontal one-half-strength Murashige and Skoog plates with or without 17-β-estradiol; then the plates were rotated 90°. Their angle realignments were measured after 24 h.

In the amiRNA lines (lines 41 and 42), treatment with 10 μM estradiol interfered strongly with the gravitropic response; particularly, the gravitropic response in line 42 was severely impaired, suggesting that root gravitropism is inhibited dose dependently (Fig. 8, A–D).

Similarly, conditional overexpression lines of *FAB1A* and *FAB1B* revealed the root gravitropic phenotype in the presence of estradiol (Fig. 8, E–H). From these data, we concluded that auxin signaling is inhibited in both the loss-of-function and gain-of-function mutations in *FAB1A/B.*

Abnormal Flower Morphology of *FAB1A* and *FAB1B* Overexpression Mutants

The constitutive overexpression lines of *FAB1A* and *FAB1B* showed abnormal phenotypes in flower and leaf organ morphology. The phenotypes were categorized into six typical types based on morphology including an ovule-like structure that appeared inside of a curled sepal (Fig. 9A), sepals with a carpel-like structure (Fig. 9B), ovule-like structures in a curled leaf (Fig. 9C), a stamen fused to the sepal (Fig. 9D), papilla that emerged on the tip of the stamen (Fig. 9E), and three flowers branching from a single place (Fig. 9F). The abnormal morphology in flowers of cFAB1B-OX

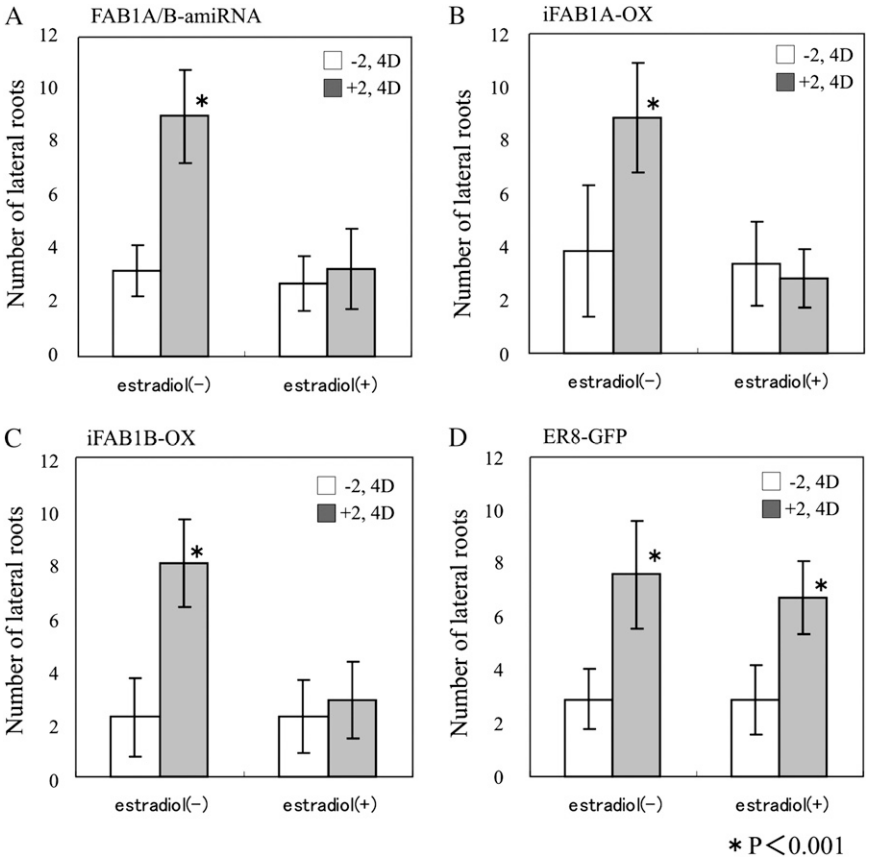

Figure 7. Knockdown and overexpressing of *FAB1A/B* become less sensitive to exogenous auxin in the lateral root formation. The number of lateral roots of the amiRNA transgenic line 42 used in Figure 3 (A), *FAB1A* overexpression line (B), *FAB1B* overexpression line (C), and a control GFP expression line (D) were counted without (white bars) or with (gray bars) 0.1 μM 2,4-D treatment in the presence of or absence of 10 μM estradiol. Bars show mean values ± SD (number of lateral roots counted: FAB1A/B-amiRNA − estradiol, $n = 100$; FAB1A/B-amiRNA + estradiol, $n = 103$; iFAB1A-OX − estradiol, $n = 87$; iFAB1A-OX + estradiol, $n = 97$; iFAB1B-OX − estradiol, $n = 96$; iFAB1B-OX + estradiol, $n = 106$; ER8-GFP − estradiol, $n = 101$; ER8-GFP + estradiol, $n = 94$). Asterisks denote statistically significant differences in the number of lateral roots compared with uninduced conditions (*$P < 0.001$; Student's t test).

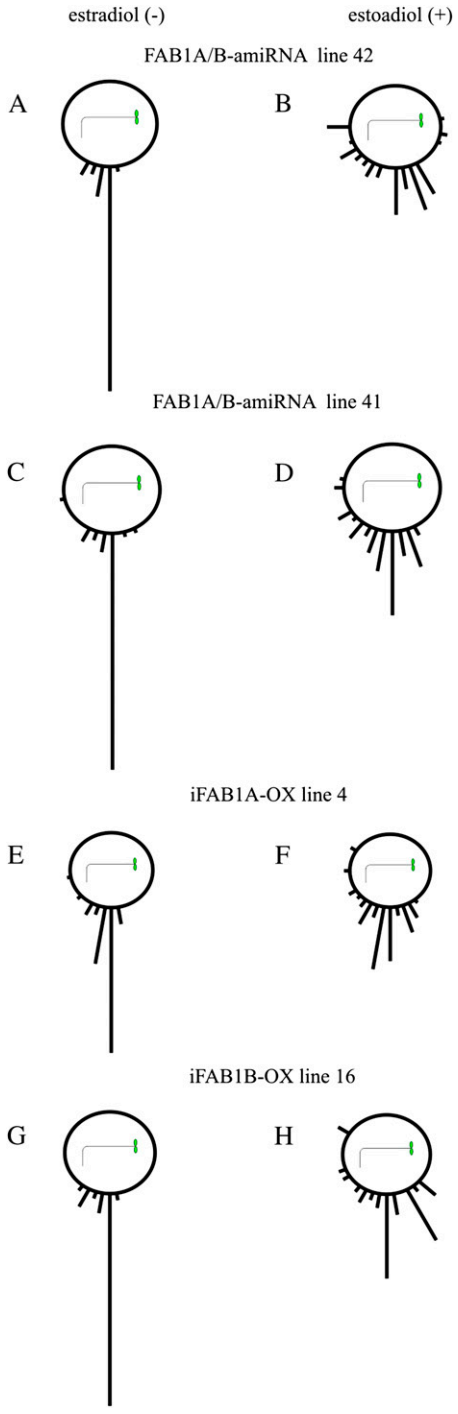

Figure 8. Root gravitropic response is impaired in *FAB1A/B* knockdown and overexpressing mutants. After the seeds of the estradiol (10 μM)-inducible knockdown transgenic plant of *FAB1A/B* (line 42 [A and B] and line 41 [C and D] used in Fig. 3), and those containing the overexpression of *FAB1A* (E and F) and *FAB1B* (G and H) were sown on the vertically placed one-half-strength Murashige and Skoog agar plates for 5 d, these plates were then rotated 90° and incubated for an additional 24 h. Then root tip curvatures were measured. Each gravity-stimulated root was assigned to a 10° sector, of which there were 36. The length of each bar represents the frequency in each degree (numbers of roots measured: FAB1A/B-amiRNA line 42 − estradiol, n = 57; FAB1A/B-amiRNA line 42 + estradiol, n = 72; FAB1A/B-amiRNA line 41 − estradiol, n = 62; FAB1A/B-amiRNA line 41 + estradiol, n = 58; iFAB1A-OX − estradiol, n = 57; iFAB1A-OX + estradiol, n = 40; iFAB1B-OX − estradiol, n = 40; iFAB1B-OX + estradiol, n = 37). [See online article for color version of this figure.]

lines resembled that in the cFAB1A-OX lines (data not shown). These floral phenotypes suggest that floral organ identity genes might be misregulated dose dependently in the *FAB1A/B* gain-of-function mutants.

DISCUSSION

In an earlier study, the functions of FAB1A and FAB1B were analyzed using the T-DNA insertional mutation lines of both genes in Arabidopsis (Whitley et al., 2009). However, because of the unavailability of *FAB1A/B* double-knockout plant, the physiological significance of FAB1A/B in vegetative tissues remains to be investigated. Here, we generated conditional knockdown and overproducing mutant plants to examine the physiological functions of FAB1A/B in vegetative tissues. Results show that FAB1A and FAB1B are important for maintenance of endomembrane homeostasis including endocytosis, vacuole formation, and vacuolar acidification processes, and impairment of FAB1A/B function caused pleiotropic developmental abnormalites in Arabidopsis.

Function of Arabidopsis FAB1A/B Proteins in Plant Cells

Introducing Arabidopsis *FAB1A* and *FAB1B* cDNAs into fission yeast *fab1* mutant (*ste12*Δ) completely complemented the enlarged vacuole phenotype of the mutant, indicating that Arabidopsis FAB1A and FAB1B fully function as the PtdIns3P-5 kinase in fission yeast, and the molecular functions are conserved through the evolution. Furthermore, conditional reduction of *FAB1A/B* expression in Arabidopsis root cells induced severe defects in the central vacuole acidification and the endocytosis process. These defects are known as common phenotypes of *fab1* mutation in yeast and animal cells (Gary et al., 1998; Odorizzi et al., 1998; McEwen et al., 1999; Ikonomov et al., 2001). Therefore, we conclude that the primary function of FAB1A and FAB1B is the endosome-resident PtdIns3P-5 kinase, FAB1/PIKfyve, in plants, just as it is in other eukaryotic organisms.

Why Do Loss-of-Function and Gain-of-Function Mutants Reveal the Same Phenotypes on Auxin Signaling?

Because the double-homozygous *fab1a/fab1b* knockout plants failed to generate any seeds because of a fatality of the pollen grains having mutations in both genes, it was impossible to analyze the biological function of *FAB1A/B* in the developmental process

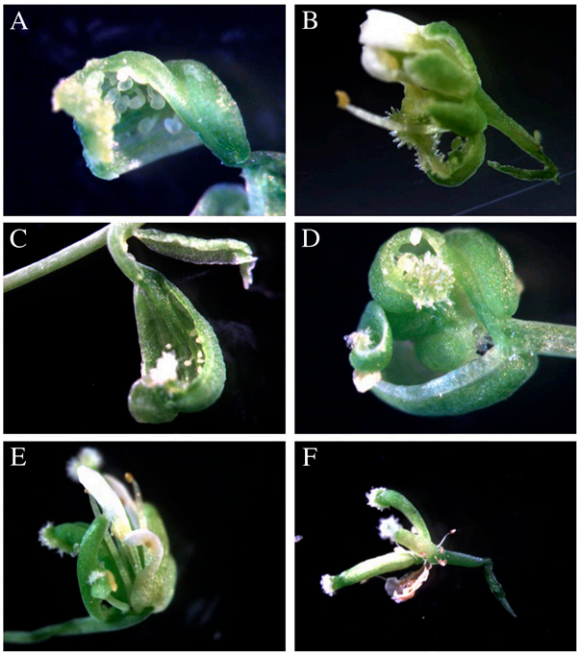

Figure 9. Transgenic plants expressing *FAB1A* represents abnormal floral organ phenotypes. Overexpression of *FAB1A* caused abnormal flower types, including ovule-like structures appearing inside of a curled sepal (A), sepals with a carpel-like structure (B), ovule-like structures in a curled leaf (C), a stamen fused to sepals (D), papilla that emerged on the stamen tip (E), and three flowers branched from a single place, as in the terminal flower phenotype (F). [See online article for color version of this figure.]

of the vegetative tissues in Arabidopsis despite the fact that only subtle leaf-curling phenotype was observed in both *fab1a* and *fab1b* single-homozygous plants (Whitley et al., 2009).

To avoid that difficulty, we generated transgenic plants that were able to reduce the expressions of *FAB1A/B* conditionally by addition of a trace amount of estradiol. We analyzed the phenotypes of the conditional loss-of-function mutation in *FAB1A/B*. Decreased expression levels of *FAB1A/B* induced various phenotypes including marked root growth inhibition, root gravitropic response, and hyposensitivity to exogenous auxin. Intriguingly, such phenotypes were also observed when *FAB1A/B* was conditionally overexpressed.

In yeast and animals, Fab1p/PIKfyve form a protein complex with Fab1 regulatory proteins, Fig4/Sac3 (a lipid phosphatase), Vac7 (a FAB1 activator) and Atg18 (a FAB1 effector), and a scaffold protein, Vac14 (Duex et al., 2006; Efe et al., 2007; Sbrissa et al., 2007; Michell and Dove, 2009). All genes encoding Fab1 complex proteins, except Vac7, have also been found in the Arabidopsis genome. The enzymatic activity of Arabidopsis FAB1 is also likely to be regulated with these FAB1-regulatory proteins in a complex form. Therefore, a possible explanation of why the *FAB1A/B* loss-of-function and gain-of-function mutants show a similar phenotype is that an imbalance in the expression of *FAB1A/B* might inhibit proper complex formation of FAB1 with its regulatory proteins, thereby disrupting precise control of PtdIns (3,5)P_2 production in response to various environmental stresses. Indeed, controlled expression of Arabidopsis FAB1A/B proteins in fission yeast *ste12* mutant that was attained by adding various concentrations of thiamine altered the vacuolar shape of the mutant dose dependently (data not shown). That result suggests that precise expression control of *FAB1* gene is important for its function.

Various Developmental Phenotypes of *fab1a/b* Mutants

Reduced expression of *FAB1A/B* causes severe defects in bulk-flow endocytosis and vacuolar acidification in root cells. These defects might cause impairment of proper endomembrane trafficking, and might consequently affect the trafficking of various regulatory molecules on the plasma membrane (PM). We observed various developmental phenotypes in the loss-of-function and gain-of-function mutants of *FAB1A/B*. Most of the phenotypes are reminiscent of the typical phenotypes observed in the auxin-resistant mutants including *aux1* (Marchant et al., 1999) and *axr4* (Hobbie and Estelle, 1995; Dharmasiri et al., 2006). AUXIN-RESISTANT1 (AUX1), which is a permease-like membrane protein, facilitates auxin uptake and mediates the directional auxin flow along with auxin efflux carriers: PIN family proteins (Swarup et al., 2004). In root apical cells, AUX1 and PIN2 are distributed on the PM in a polarized fashion. Polar distributions of AUX1 and PINs on the PM are established by constitutive recycling among the endosomes and the particular domain of the PM (Friml, 2010). Intriguingly, *aux1* and *pin2* mutants share the same mutant phenotype on the root gravitropic response (Marchant et al., 1999; Shin et al., 2005), indicating that that the two auxin transporters mutually act together to mediate directional auxin flow to establish root gravitropism. The defect in the endocytosis process in *fab1a/b* mutants might inhibit precise recycling of these auxin carriers, thereby perturbing regulated auxin flow mediated by these auxin carrier proteins, consequently causing the pleiotropic auxin-signaling phenotypes.

Therefore, most phenotypes of *fab1* mutants reported here are explainable by defects in recycling of such auxin transporters, although several morphological phenotypes including floral organ abnormality and pollen developmental defect remain elusive. It is likely that the trafficking of other important developmental regulators on the PM is affected in the *fab1a/b* mutant lines. For instance, the Leu-rich receptor-like Ser/Thr kinase (LRR-RLK) super family constitutes over 600 coding genes involved in a wide variety of signaling processes in Arabidopsis (Shiu and Bleecker, 2003). One subfamily of LRR-RLKs, ERECTA-family receptor-like kinases, controls organ growth and flower development in Arabidopsis. Loss of all ERECTA family genes led to striking dwarfism, reduced lateral organ size, and abnormal flower development (Shpak

et al., 2003). In *fab1* mutants, mislocalization of these receptors can occur, thereby causing abnormal morphology in flower organs. In this study, we could not rule out the possibility that endocytosis of the PM proteins are nonspecifically impaired in *fab1a/b* mutants. Future studies should investigate sorting defects of these regulatory proteins on the PM in *fab1a/b* mutants.

MATERIALS AND METHODS

Plant Growth Conditions

Arabidopsis (*Arabidopsis thaliana*) ecotype Columbia was used for all experiments described herein. Plants were grown under white light with 16-h-light and 8-h-dark cycles at 22°C.

Plasmid Construction

Arabidopsis cDNAs were synthesized using AMV reverse transcriptase (Takara) from total RNA isolated from Arabidopsis seedlings using an RNeasy mini kit (Qiagen Inc.). The open reading frames of *FAB1A* (At4g33240) and *FAB1B* (At3g14270) were amplified using PCR with KOD-FX DNA polymerase (Toyobo Co.) with Arabidopsis cDNAs as a template with appropriate primers. The amplified fragments were subcloned into pENTR (Invitrogen Corp.). Then the inserted fragments were verified with sequencing. The upstream untranslated regions of *FAB1A* (1,787 bp) and *FAB1B* (3,166 bp) were amplified from the Arabidopsis genome. Then each amplified upstream region was fused into each cDNA construct in pENTR to generate own-promoter-driven *FAB1A/B* cDNA constructs. The constructs were transferred into a binary vector, pGWB504 (Nakagawa et al., 2007), using the Gateway cloning method to generate C-terminally GFP-fused constructs. The constructs were designated, respectively, as FAB1A/pGWB504 and FAB1B/pGWB504.

For constructing vectors for the constitutive and conditional expression of *FAB*1A/*B*, *FAB*1A/*B* full-length cDNAs were subcloned, respectively, into pGWB502 (Nakagawa et al., 2007) and pER8 (Zuo et al., 2000) to generate FAB1A/pGWB502, FAB1B/pGWB502, FAB1A/pER8, and FAB1B/pER8.

For generating the amiRNA construct for inhibiting the expressions of *FAB1A* and *FAB1B* simultaneously, we designed an optimal amiRNA sequence using software (WMD version 3; http://wmd.weigelworld.org/). The designed target 21-mers amiRNA sequence (5′-TAACTCCATACTGGATCGCAT-3′) was synthesized using the following primers: (miRNA-sense, 5′-gaTAACTCCATACTGGATCGCATctctctctttgtattcc-3′; miRNA-antisense, 5′-gaATGCGATCCAGTATGGAGTTAtcaaagagaatcaatga-3′; miRNA*-sense, 5′-gaATACGATCCAGTAAGGAGTTTtcacaggtcgtgatatg-3′; miRNA*-antisense, 5′-gaAAACTCCTTACTGGATCGTATtctacatatatattcct-3′; primer-A, 5′-CACCCTGCAAGGCGATTAAGTTGGGTAAC-3′; primer-B, 5′-GCGGATAACAATTTCACACAGGAAACA-3′) according to the method described in Schwab et al. (2006) and Ossowski et al. (2008). The amplified amiRNA fragment was then introduced into the pER8 vector to generate FAB1A/B-amiRNA/pER8. The transgenic plant conditionally expressing GFP (ER8-GFP) was used as a mock control (Kusano et al., 2008). Constructed plasmids and generating transgenic plants used in this study are listed in Supplemental Table S1.

Agrobacterium Transformation and Generating Transgenic Plants

The binary constructs were introduced into *Agrobacterium tumefaciens* strain GV3101 by electroporation; then Arabidopsis wild-type plants (Columbia-0) were transformed by the floral-dipping method (Clough and Bent, 1998). Screening of transgenic plants was performed on one-half-strength Murashige and Skoog plates containing 50 $\mu g \cdot mL^{-1}$ hygromycin. The names and numbers of generating transgenic plants are also listed in Supplemental Table S1.

Complementation Assay in Fission Yeast

Fission yeast (*Schizaccharomyces pombe*), an *ste12* mutant, M879-3H (*h*^{90} *ste12*::*ura4*$^{+}$ *ade6-M210 ura4-D18 leu1*; Morishita et al., 2002) was used for this study. The full-length cDNAs of *FAB1A* and *FAB1B* were introduced into pREP41 having the thiamine-repressible *nmt* promoter (Maundrell, 1993). For induction of Arabidopsis *FAB1A/B* expression, thiamine was depleted from the medium.

FM4-64 Staining

Yeast (*Saccharomyces cerevisiae*) cells were harvested and then labeled with 2 μM of the endocytosis marker, FM4-64 [*N*-(3-triethylammoniumpropyl)-4-(p-diethylaminophenol) pyridinium dibromide]. Arabidopsis roots were labeled by soaking for 10 min in 2 μM FM4-64 solution.

Acridine Orange Treatment

Acridine orange (Sigma-Aldrich Corp.) was added to 5-d-old seedlings of conditional loss-of-function and gain-of-function mutants to a final concentration of 50 μM. After incubation at room temperature in the dark for 100 min, the seedlings were washed twice with water. They were then observed using confocal microscopy.

Confocal Microscopy

GFP fluorescence signals and differential interference contrast (DIC) images were obtained using a laser-scanning microscope (Eclipse E600; Nikon Instruments Co.) equipped with the C1si ready confocal system (Nikon). The collected images were processed using image analysis software (EZ-C1; Nikon).

Pollen Analysis

Pollen viability was assayed by staining pollen grains with 0.5 $\mu g \cdot mL^{-1}$ FDA. The pollen vacuoles were visualized by staining with 0.02% (w/v) neutral red in 8% (w/v) Suc.

Semiquantitative RT-PCR

Total RNA was extracted from the transgenic lines. Then RT was performed using reverse transcriptase XL (Takara) using 2 μg of total RNA as a template with an oligo-d(T)$_{20}$ and random primer mixture for 1 h at 42°C. Of the reaction mixture, 1 μL was taken for a subsequent PCR reaction. The Arabidopsis *FAB1A/B* and *ACTIN-2* (At3g18780) cDNAs were amplified with an annealing temperature of 50°C during 25 cycles. Primer pairs used in the RT-PCR reaction were Fab1A-F (5′-AAGCCAGATACAAGTAAAAGTGGAG-3′) and Fab1A-R (5′-AAACAACTCCTTTCACGACCA-3′) for *Fab1A*, Fab1B-F (5′-TGGATCAAAACTTGATTGAAGC-3′) and Fab1B-R (5′-ATCCATCACATCACCCAATG-3′) for *FAB1B*, and ACT2-F (5′-CCGCTCTTTCTTTCCAAGC-3′) and ACT2-R (5′-CCGGTACCATTGTCACACAC-3′) for *ACTIN-2*.

Measurement of Root Length

Roots were observed in 5-d-old seedlings grown on one-half-strength Murashige and Skoog agar plates containing 10 μM 17-β-estradiol. Their lengths were measured using image analysis software (ImageJ; National Institutes of Health).

Sequence data from this article can be found in the GenBank/EMBL data libraries under accession numbers NM_119478 and NM_112285.

Supplemental Data

The following materials are available in the online version of this article.

Supplemental Fig. S1. Root hair development is inhibited in conditional FAB1A/B-amiRNA, iFAB1A-OX, and iFAB1B-OX mutants.

Supplemental Fig. S2. Overexpression of *FAB1A* or *FAB1B* inhibits pollen development.

Supplemental Fig. S3. Reduction of *FAB1A/B* expression delays endocytosis.

Supplemental Table S1. List of constructs used for this study.

ACKNOWLEDGMENTS

We thank N.H. Chua (Rockefeller University, United States), T. Aoyama (Kyoto University, Japan), and T. Nakagawa (Shimane University, Japan) for providing pER8, ER8-GFP, and pGWB502/504, respectively. We also thank T. Fujiki (Saitama University, Japan) and K. Ichihara (Kyoto Prefectural University, Japan) for their helpful insights and M. Ichikawa (Kyoto Prefectural University, Japan) for technical assistance.

Received October 21, 2010; accepted December 14, 2010; published December 20, 2010.

LITERATURE CITED

Alvarez JP, Pekker I, Goldshmidt A, Blum E, Amsellem Z, Eshed Y (2006) Endogenous and synthetic microRNAs stimulate simultaneous, efficient, and localized regulation of multiple targets in diverse species. Plant Cell **18:** 1134–1151

Clough SJ, Bent AF (1998) Floral dip: a simplified method for Agrobacterium-mediated transformation of *Arabidopsis thaliana*. Plant J **16:** 735–743

Dharmasiri S, Swarup R, Mockaitis K, Dharmasiri N, Singh SK, Kowalchyk M, Marchant A, Mills S, Sandberg G, Bennett MJ, et al (2006) AXR4 is required for localization of the auxin influx facilitator AUX1. Science **26:** 1218–1220

Duex JE, Tang F, Weisman LS (2006) The Vac14p-Fig4p complex acts independently of Vac7p and couples $PI3,5P_2$ synthesis and turnover. J Cell Biol **172:** 693–704

Efe JA, Botelho RJ, Emr SD (2005) The Fab1 phosphatidylinositol kinase pathway in the regulation of vacuole morphology. Curr Opin Cell Biol **17:** 402–408

Efe JA, Botelho RJ, Emr SD (2007) Atg18 regulates organelle morphology and Fab1 kinase activity independent of its membrane recruitment by phosphatidylinositol 3,5-bisphosphate. Mol Biol Cell **18:** 4232–4244

Friml J (2010) Subcellular trafficking of PIN auxin efflux carriers in auxin transport. Eur J Cell Biol **89:** 231–235

Gary JD, Wurmser AE, Bonangelino CJ, Weisman LS, Emr SD (1998) Fab1p is essential for PtdIns(3)P 5-kinase activity and the maintenance of vacuolar size and membrane homeostasis. J Cell Biol **143:** 65–79

Hobbie L, Estelle M (1995) The *axr4* auxin-resistant mutants of *Arabidopsis thaliana* define a gene important for root gravitropism and lateral root initiation. Plant J **7:** 211–220

Ikonomov OC, Sbrissa D, Shisheva A (2001) Mammalian cell morphology and endocytic membrane homeostasis require enzymatically active phosphoinositide 5-kinase PIKfyve. J Biol Chem **276:** 26141–26147

Kusano H, Testerink C, Vermeer JEM, Tsuge T, Shimada H, Oka A, Munnik T, Aoyama T (2008) The *Arabidopsis* phosphatidylinositol phosphate 5-kinase PIP5K3 is a key regulator of root hair tip growth. Plant Cell **20:** 367–380

Marchant A, Kargul J, May ST, Muller P, Delbarre A, Perrot-Rechenmann C, Bennett MJ (1999) AUX1 regulates root gravitropism in Arabidopsis by facilitating auxin uptake within root apical tissues. EMBO J **18:** 2066–2073

Maundrell K (1993) Thiamine-repressible expression vectors pREP and pRIP for fission yeast. Gene **123:** 127–130

McEwen RK, Dove SK, Cooke FT, Painter GF, Holmes AB, Shisheva A, Ohya Y, Parker PJ, Michell RH (1999) Complementation analysis in PtdInsP kinase-deficient yeast mutants demonstrates that *Schizosaccharomyces pombe* and murine Fab1p homologues are phosphatidylinositol 3-phosphate 5-kinases. J Biol Chem **274:** 33905–33912

Michell RH, Dove SK (2009) A protein complex that regulates PtdIns(3,5)P2 levels. EMBO J **28:** 86–87

Morishita M, Morimoto F, Kitamura K, Koga T, Fukui Y, Maekawa H, Yamashita I, Shimoda C (2002) Phosphatidylinositol 3-phosphate 5-kinase is required for the cellular response to nutritional starvation and mating pheromone signals in *Schizosaccharomyces pombe*. Genes Cells **7:** 199–215

Nakagawa T, Kurose T, Hino T, Tanaka K, Kawamukai M, Niwa Y, Toyooka K, Matsuoka K, Jinbo T, Kimura T (2007) Development of series of gateway binary vectors, pGWBs, for realizing efficient construction of fusion genes for plant transformation. J Biosci Bioeng **104:** 34–41

Niu QW, Lin SS, Reyes JL, Chen KC, Wu HW, Yeh SD, Chua NH (2006) Expression of artificial microRNAs in transgenic *Arabidopsis thaliana* confers virus resistance. Nat Biotechnol **24:** 1420–1428

Odorizzi G, Babst M, Emr SD (1998) Fab1p PtdIns(3)P 5-kinase function essential for protein sorting in the multivesicular body. Cell **95:** 847–858

Ossowski S, Schwab R, Weigel D (2008) Gene silencing in plants using artificial microRNAs and other small RNAs. Plant J **53:** 674–690

Sbrissa D, Ikonomov OC, Fu Z, Ijuin T, Gruenberg J, Takenawa T, Shisheva A (2007) Core protein machinery for mammalian phosphatidylinositol 3,5-bisphosphate synthesis and turnover that regulates the progression of endosomal transport: novel Sac phosphatase joins the ArPIKfyve-PIKfyve complex. J Biol Chem **282:** 23878–23891

Schwab R, Ossowski S, Riester M, Warthmann N, Weigel D (2006) Highly specific gene silencing by artificial microRNAs in *Arabidopsis*. Plant Cell **18:** 1121–1133

Shaw JD, Hama H, Sohrabi F, DeWald DB, Wendland B (2003) PtdIns(3,5) P2 is required for delivery of endocytic cargo into the multivesicular body. Traffic **4:** 479–490

Shin H, Shin H-S, Guo Z, Blancaflor EB, Masson PH, Chen R (2005) Complex regulation of Arabidopsis AGR1/PIN2-mediated root gravitropic response and basipetal auxin transport by cantharidin-sensitive protein phosphatases. Plant J **42:** 188–200

Shiu SH, Bleecker AB (2003) Expansion of the receptor-like kinase/Pelle gene family and receptor-like proteins in Arabidopsis. Plant Physiol **132:** 530–543

Shpak ED, Berthiaume CT, Hill EJ, Torii KU (2003) Synergitic interaction of three ERECTA-family receptor-like kinases controls Arabidopsis organ growth and flower development by promoting cell proliferation. Development **131:** 1491–1501

Swarup R, Kargul J, Marchant A, Zadik D, Rahman A, Mills R, Yemm A, May S, Williams L, Millner P, et al (2004) Structure-function analysis of the presumptive *Arabidopsis* auxin permease AUX1. Plant Cell **16:** 3069–3083

Warthmann N, Das S, Lanz C, Weigel D (2008) Comparative analysis of the MIR319a microRNA locus in Arabidopsis and related *Brassicaceae*. Mol Biol Evol **25:** 892–902

Whitley P, Hinz S, Doughty J (2009) Arabidopsis FAB1/PIKfyve proteins are essential for development of viable pollen. Plant Physiol **151:** 1812–1822

Zuo J, Niu QW, Chua NH (2000) Technical advance: an estrogen receptor-based transactivator XVE mediates highly inducible gene expression in transgenic plants. Plant J **24:** 265–273